Electronic Supplementary Material (ESI) for RSC Advances.

Supporting Information

One-step thermal polymerization synthesis of nitrogen-rich g-C_3N_4 nanosheets enhances photocatalytic redox activity

Leyu Peng,[a] Jiaxi Liu,[a,b] Ziyuan Li,[a] Yifan Jing,[a] Yongjin Zou,[a] Hailiang Chu,[a] Fen Xu,[a] Lixian Sun,*[a,b] and Pengru Huang*[a]

Experimental section

Characterizations

The characterization test equipment used in this experiment is as follows: X-ray powder diffractometer (XRD; Cu Kα radiation, Bruker DAVINCI D8 ADVANCE diffractometer) were analyzed the crystal structure; X-ray Photoelectron Spectrometer (XPS; ESCALAB 250Xi, Thermo Fisher) analyzed elemental compositions and chemical states; Fourier Transform Infrared Measurements (FTIR; 6700, Nicolet) spectra to use analyze surface functional groups; Scanning electron microscope (SEM; Quanta 200, FEI) and transmission eletron microscope (TEM; Talos F200X, FEI Company, USA) ~~was~~were observed the surface morphology; Diffuse reflectance ultraviolet-visible spectra (UV-vis DRS; Metash UV-8000) were collected the visible light absorption information with $BaSO_4$ reference; Brunauer-Emmett-Teller (BET; Autosorb iQ2, Quantachrome, USA) were determined specific surface areas and pore structure of all the samples; The steady photoluminescence (PL) spectra and time-correlated single-photon counting (TCSPC) were measured under 310 nm excitation; Electron Spin Resonance (ESR) spectra of samples were measured on a ESR spectrometer (Bruker EMX PLUS, Germany), after dispersing 2 mg sample into mixture of 100 μl deionized water containing 20 μl 5,5-dimethyl-1-pyrrolidine N-oxide (DMPO) of 0.19 M and irradiated for 10 min under visible light ($\lambda > 420$ nm), for detection of •OH.

The photo-electrochemical (EIS and TPS) were conducted on an electrochemical workstation (CHI 660E,) employing a three-electrode system (a Pt counter electrode, an Ag/AgCl reference electrode, and a working electrode). The working electrode was prepared as follows: 2 mg of samples were dispersed in a mixed solution which includes 100 μL of ethyl alcohol and 5 μL of Nafion and sonicated for an hour; then the slurry was equally dip-coated onto ITO glass and dried.

Photocatalytic activity measurement

Rhodamine B (RhB) was selected as the target pollutant in photo-degradation experiments. 10 mg photocatalysts were scattered to 50 ml RhB solution (20 ppm). The catalyst was first adsorbed in the dark for 30 minutes before visible light irradiation (300 W Xenon lamp, $\lambda > 420$ nm), after that, every 10 min interval, 4 ml of the suspension were extracted and centrifuged to obtain the supernatant. And the solution was analyzed through a UV-vis spectrophotometer (UV-8000, ranging from 380-700 nm).

The H_2 evolution activity of different samples was tested to study the photocatalytic reduction activity. 20 mg photocatalysts were firstly dispersed into a 100 ml solution (20% volume TEOA and 160 μl 10 mg/ml $H_2PtCl_6 \cdot 6H_2O$), the resulting suspension was degassed for 30 min (vacuum condition), and then photo-deposition was used to prepare the catalyst with supported Pt. After degassing again for 30 min to eliminate residual gas, then periodically sample the H_2 generation.

Calculations of density functional theory (DFT)

All the theoretical calculations were performed based on the density functional theory (DFT) by means of the Vienna Ab-initio Simulation Package (VASP), with the projected augmented wave (PAW) method.[1] The Perdew-Burke-Ernzerhof (PBE) functional within the generalized gradient approximation (GGA) is used to describe the exchange-correlation potential.[2-3] The van der Waals was considered via Grimme's DFT-D3 method. The kinetic energy cutoff is set to 500 eV. During the geometry optimizations, the convergence criteria for force and energy were set to 0.02 eV/Å and 1×10^{-5} eV, respectively. The vacuum layer was set to 20 Å. The Brillouin-zone was sampled by the gamma-centered Monkhorst-Pack method with a 5×5×1 k-point mesh.

Results

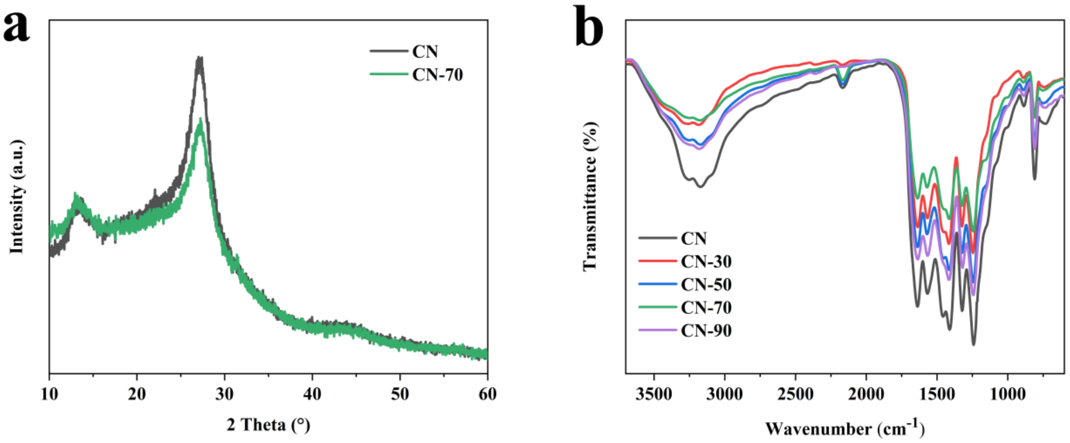

Fig. S1(a) The XRD patterns of CN and CN-70 (b) The FT-IR spectra peak intensity of all the samples.

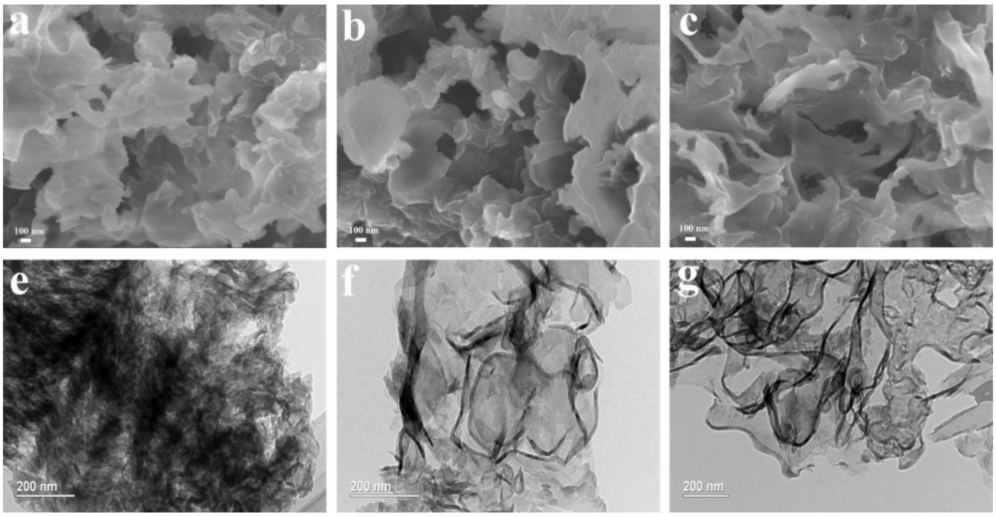

Fig.S2 The SEM images of (a) CN, (b)-(c) CN-70 and TEM images of (e) CN, (f)-(g) CN-70.

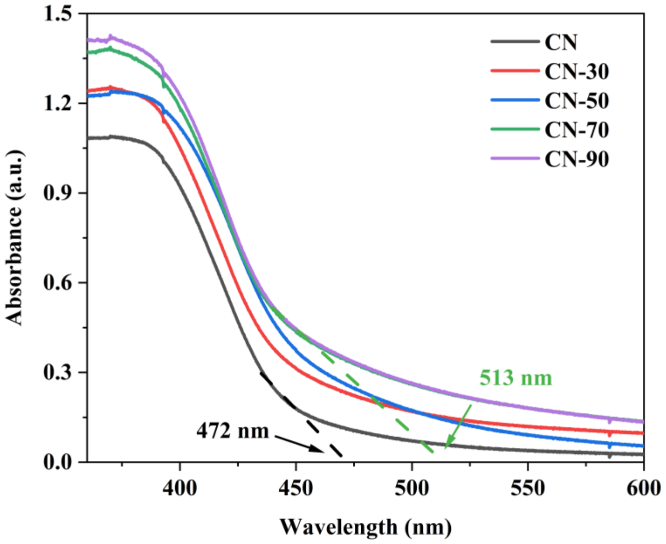

Fig. S3 The UV-vis DRS spectra of all the samples.

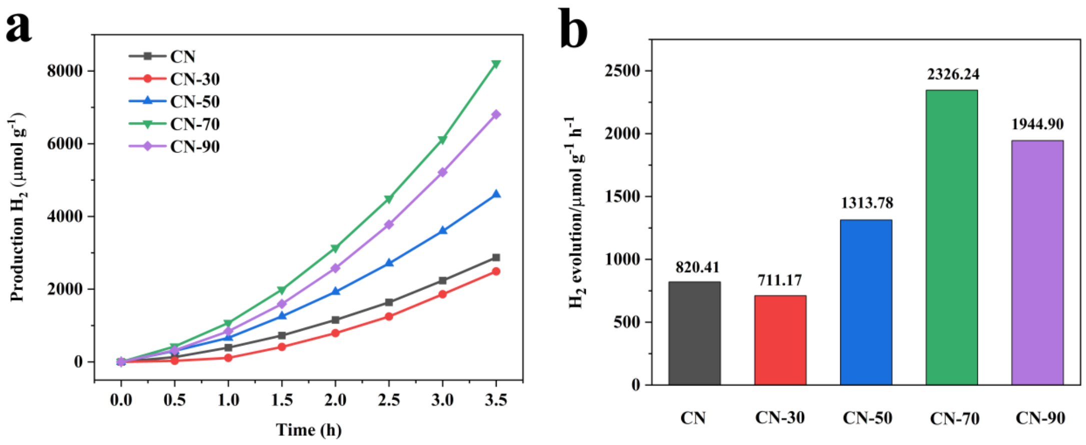

Fig. S4 (a) Amount of H_2 generation (b) H_2 generation rate of the CN and CN-X.

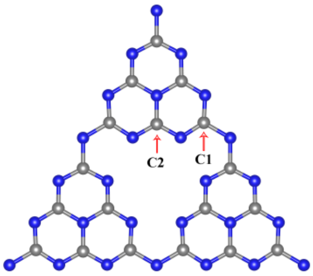

Fig. S5 Structural model of g-C_3N_4 (CN) with two possible C sites(C and N are indicated by grey and blue spheres).

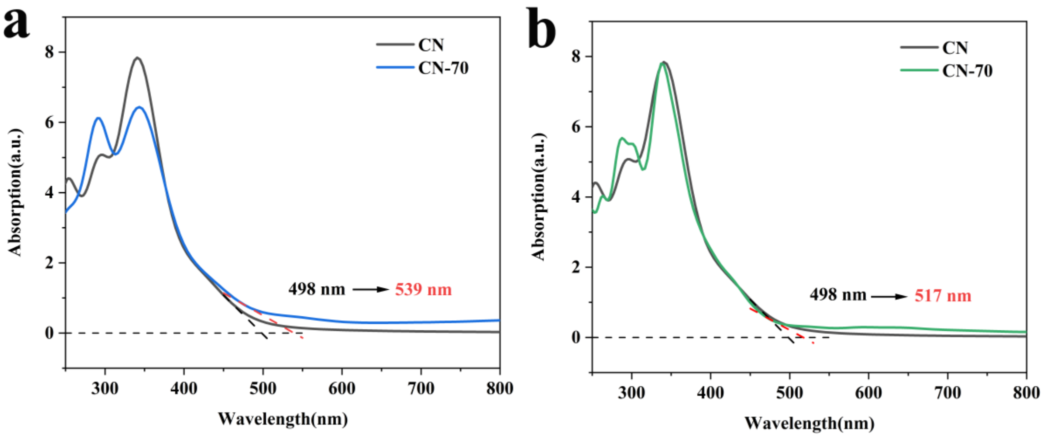

Fig. S6 Calculations of the visible light absorption spectrum of (a) CN-70(C1) and (b) CN-70(C2).

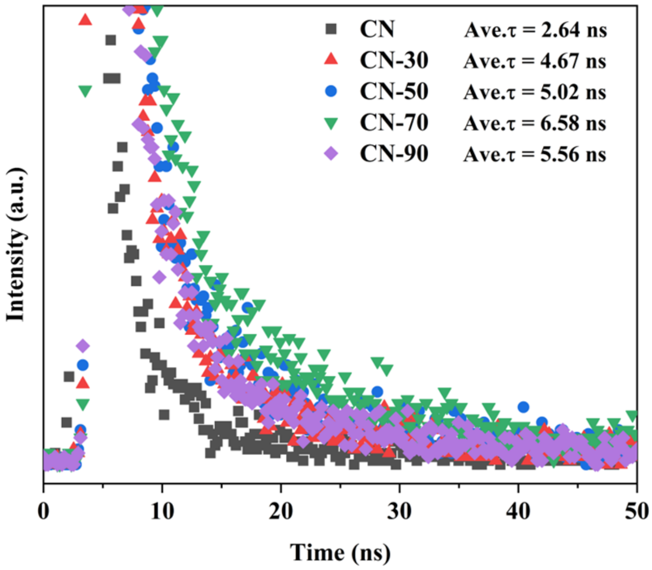

Fig.S7 The transient PL of CN and CN-X.

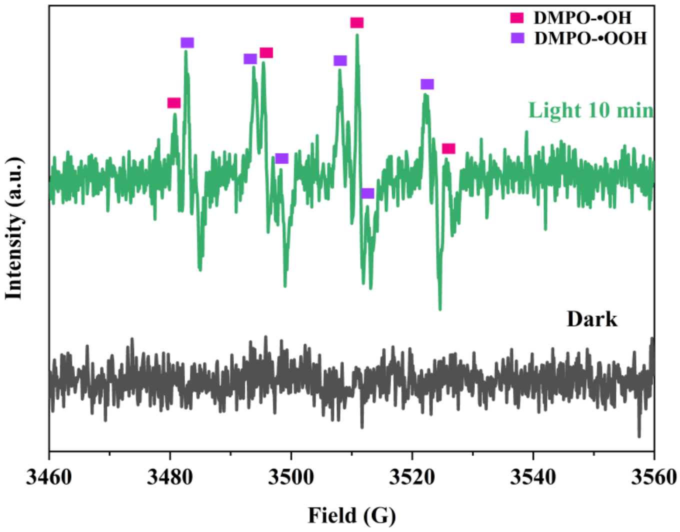

Fig.S8 The ESR results of CN-70 in the darkness and visible light irradiation.

Table S1. Specific surface area, pore size distribution and pore volume of samples

Sample	**Surface area (m^2/g)**	**Pore diameter (nm)**	**Pore volume (cm^3/g)**
CN	58.499	21.982	0.321
CN-30	77.205	28.055	0.551
CN-50	83.875	25.934	0.544
CN-70	86.532	36.263	0.784
CN-90	79.436	31.260	0.621

Table S2. XPS analysis of C1s for CN and CN-70

Sample	**C-C/C=C**	**N=C-N**
CN	52.46%	47.54%
CN-70	37.62%	62.38%

Table S3. XPS analysis of N1s for CN and CN-70

Sample	**C-N=C**	**N_3C-low binding energy**	**N_3C-high binding energy**	**$-NH_2$/N-N**
CN	58.13%	21.94%	11.17%	8.36%
CN-70	62.13%	16.22%	11.91%	9.74%

Table S4. Fitting results of the photoluminescence decay time

Sample	**τ1/ns**	**Rel%**	**τ2/ns**	**Rel%**	**average τ/ns**
CN	0.8596	54.15	4.7451	45.85	2.6411
CN-30	1.4046	56.85	8.9684	43.15	4.6684
CN-50	1.4659	57.28	9.7911	42.72	5.0224
CN-70	1.6945	52.35	11.9531	47.65	6.5827
CN-90	1.4817	57.87	11.1571	42.13	5.5579

Table S5. RhB degradation rate of g-C_3N_4 based photocatalysts reported by literature.

Photocatalysts	**Light source**	**Reaction conditions**	**RhB degradation rate k (min^{-1})**	**Ref.**
P@P-g-C_3N_4	λ > 420 nm	50mg 100ml 10mg/l	0.0659	[4]
60-C_3N_4	λ > 420 nm	12mg 60ml 10mg/l	0.0434	[5]
1D/2D O-doped g-C_3N_4	λ > 420 nm	100mg 100ml 30mg/l	0.0551	[6]
SN-GQDs/g-C_3N_4	λ > 420 nm	50mg 100ml 5mg/l	0.0388	[7]
Porous-g-C_3N_4	λ > 420 nm	10mg 50ml 10mg/l	0.04559	[8]
few-layered porous g-C_3N_4	λ > 420 nm	25mg 50ml 10mg/l	0.027	[9]
CN-70	λ > 420 nm	10mg 50ml 20mg/l	0.06274	This work

Table S6. The H_2 evolution rate of g-C_3N_4 based photocatalysts reported by literature.

Photocatalysts	**Light source**	**Reaction conditions**	**H_2 evolution rate (μmol/g/h)**	**Ref.**
P@P-g-C_3N_4	λ > 420 nm	3 wt% Pt, TEOA (10 vol%)	941.80	[4]
few-layered porous g-C_3N_4	λ > 420 nm	3 wt% Pt, TEOA (10 vol%)	304	[8]
SS-CN	λ > 420 nm	1 wt% Pt, TEOA (10 vol%)	982.33	[10]
BP-g-C_3N_4	λ > 420 nm	1 wt% Pt, TEOA (10 vol%)	1900	[11]
K-doped g-C3N4	λ > 420 nm	3 wt% Pt, TEOA (10 vol%)	1337	[12]
few-layer C_3N_4	λ > 420 nm	3 wt% Pt, TEOA (10 vol%)	159.8	[13]
CN-70	λ > 420 nm	3 wt% Pt, TEOA (10 vol%)	2326.24	This work

References

1 J. P. Perdew, K. Burke and M. Ernzerhof, Phys. Rev. Lett., 1996, 77(18), 3865–3868.

2 Raziq. F, Hayat. A, Humayun. M, et al. Appl. Catal. B-Environ., 2020, 270, 118867.

3 She. X, Liu. L, Ji. H, M. Li, Y. Huang, L, Du, D. Xu, H. Li, H et al. *Appl. Catal. B-Environ.,* 2016, **187,** 144-153.

4 J. Feng, D. Zhang, H. Zhou, M. Pi, X. Wang, S. Chen, *ACS Sustain. Chem. Eng.,* 2018, **6,** 6342-6349.

5 C. Feng, L. Tang, Y. Deng, J. Wang, Y. Liu, X. Ouyang, H. Yang, J. Yu, J. Wang, *Appl Catal. B-Environ.,* 2021, **281,** 119539.

6 Y. Wen, D. Qu, L. An, X. Gao, W. Jiang, D. Wu, D. Yang, Z. Sun, *ACS Sustain Chem. Eng.,* 2018, **7,** 2343-2349.

7 Cai A, Wang Q, Chang Y, Wang X. *J. Alloys. Compds.,* 2017, **692,** 183-189.

8 Y. Xiao, G. Tian, W. Li, Y. Xie, B. Jiang, C. Tian, D. Zhao, H. Fu, *J. Am. Chem. Soc.,* 2019, **141,** 2508-2515.

9 Y. Wen, D. Qu, L. An, X. Gao, W. Jiang, D. Wu, D. Yang, Z. Sun, *ACS Sustain Chem. Eng.,* 2018, **7,** 2343-2349.

10 M. Cao, K. Wang, I. Tudela, X. Fan, *Appl. Surf. Sci.,* 2021, **536,** 147784.

11 Hu. P, Chen. C, Zeng. R., Xiang. J, Huang. Y, Hou. D, Li. Q, and Huang. Y., *Nano Energy.,* 2018, **50,** 376-382.

12 Wang. Y, Zhao. S., Zhang. Y., Fang. J., Zhou. Y., Yuan. S., Zhang. C. and Chen. W, *Appl. Surf. Sci.,* 2018, **440,** 258-265.

13 Fei. B, Tang. Y, Wang. X, Dong. X, Liang. J, Fei. X, Xu. L, Song. Y. and Zhang. F, *Mater. Res. Bull.,* 2018, **102,** 209-217.